Molecular Plant
Research Article

CellPress
PARTNER JOURNAL

Phosphorylation of LTF1, an MYB Transcription Factor in *Populus*, Acts as a Sensory Switch Regulating Lignin Biosynthesis in Wood Cells

Jinshan Gui[1,*], Laifu Luo[1,3], Yu Zhong[1,2], Jiayan Sun[1], Toshiaki Umezawa[4] and Laigeng Li[1,*]

[1]National Key Laboratory of Plant Molecular Genetics and CAS Center for Excellence in Molecular Plant Sciences, Shanghai Institute of Plant Physiology and Ecology, Chinese Academy of Sciences, Shanghai 200032, China

[2]University of the Chinese Academy of Sciences, Beijing 100049, China

[3]School of Life Science, Lanzhou University, Lanzhou 730000, China

[4]Research Institute for Sustainable Humanosphere, Kyoto University, Uji, Kyoto 611-0011, Japan

***Correspondence: Jinshan Gui (jsgui@sibs.ac.cn), Laigeng Li (lgli@sibs.ac.cn)**

https://doi.org/10.1016/j.molp.2019.05.008

ABSTRACT

Lignin is specifically deposited in plant secondary cell walls, and initiation of lignin biosynthesis is regulated by a variety of developmental and environmental signals. However, the mechanisms governing the regulation of lignin biosynthesis remain to be elucidated. In this study, we identified a lignin biosynthesis-associated transcription factor (LTF) from *Populus*, LTF1, which binds the promoter of a key lignin biosynthetic gene encoding 4-coumarate-CoA ligase (4CL). We showed that LTF1 in its unphosphorylated state functions as a regulator restraining lignin biosynthesis. When LTF1 becomes phosphorylated by PdMPK6 in response to external stimuli such as wounding, it undergoes degradation through a proteasome pathway, resulting in activation of lignification. Expression of a phosphorylation-null mutant version of LTF1 led to stable protein accumulation and persistent attenuation of lignification in wood cells. Taken together, our study reveals a mechanism whereby LTF1 phosphorylation acts as a sensory switch to regulate lignin biosynthesis in response to environmental stimuli. The discovery of novel modulators and mechanisms modifying lignin biosynthesis has important implications for improving the utilization of cell-wall biomass.

Key words: lignin, *Populus*, secondary xylem, cell wall

Gui J., Luo L., Zhong Y., Sun J., Umezawa T., and Li L. (2019). Phosphorylation of LTF1, an MYB Transcription Factor in *Populus*, Acts as a Sensory Switch Regulating Lignin Biosynthesis in Wood Cells. Mol. Plant. **12**, 1325–1337.

INTRODUCTION

Lignin, a phenylpropanoid polymer, is an important component of the secondary cell walls (SCWs) of vascular plants (Whetten and Sederoff, 1995). The biosynthesis of lignin, which is deposited within the SCWs of specific cell types, is controlled by developmental signals and environmental stimuli, such as light, wounding, and pathogen infection (Vanholme et al., 2010; Xie et al., 2018). While general lignin biosynthetic pathways and their components have been well studied (Boerjan et al., 2003), more questions remain in elucidating specific mechanisms that effectively result in the activation or termination of lignin biosynthesis.

A hierarchical network of transcriptional activators and repressors of secondary cell-wall formation has been identified in *Arabidopsis* (Zhong and Ye, 2007; Zhong et al., 2008). The NAC transcription factors SND1/NST3, NST1, VND6, and VND7 act as the first tier of regulators that control the expression of genes involved in the biosynthesis of lignin and other SCW compounds in different cell types (Kubo et al., 2005; Zhong et al., 2006, 2007; Mitsuda et al., 2007). Members of the MYB family of transcriptional activators (MYB58, MYB63, and MYB85) and repressors (MYB4, MYB32, and other R2R3-MYB factors) have also been shown to regulate lignin formation in *Arabidopsis* (Tamagnone et al., 1998; Jin et al., 2000; Zhong et al., 2008; Zhou et al., 2009). Additional transcription factors have been cataloged across various other plant species. The snapdragon (*Antirrhinum majus*) transcription factors AmMYB308 and AmMYB330 were reported to repress lignin biosynthesis in tobacco (Tamagnone et al., 1998). In addition, *ZmMYB11*, *ZmMYB31*, and *ZmMYB42* in maize (*Zea mays*)

Published by the Molecular Plant Shanghai Editorial Office in association with Cell Press, an imprint of Elsevier Inc., on behalf of CSPB and IPPE, SIBS, CAS.

(Sonbol et al., 2009; Fornale et al., 2010; Velez-Bermudez et al., 2015), *PvMYB4* in switchgrass (*Panicum virgatum*) (Shen et al., 2012), *EgMYB1* in eucalyptus (*Eucalyptus gunnii*) (Legay et al., 2010), and *PtoMYB156* in poplar (*Populus tomentosa*) (Yang et al., 2017) have also been reported to be involved in regulation of the expression of lignin biosynthesis genes.

Protein phosphorylation, a form of post-translational modification, functions as a molecular device regulating protein location, interactions, activity, and stability (Whitmarsh and Davis, 2000). Mitogen-activated protein kinases (MAPKs or MPKs) catalyze protein phosphorylation and act in signaling cascades to link the perception of stimuli to cellular responses (Hamel et al., 2006; Colcombet and Hirt, 2008). The activated MPK can subsequently phosphorylate various substrate proteins involved in diverse biological processes (Colcombet and Hirt, 2008; Popescu et al., 2009). For example, AtMYB75 (PRODUCTION OF ANTHOCYANIN PIGMENT1, PAP1), a positive regulator of anthocyanin biosynthesis and a negative regulator of stem lignin biosynthesis (Borevitz et al., 2000; Bhargava et al., 2010), is phosphorylated by MPK4, causing an increase in its stability, which is required for light-induced anthocyanin accumulation (Li et al., 2016). In loblolly pine (*Pinus taeda*), PtMYB4 (a homolog of AtMYB46) is an activator and its phosphorylation by a MAPK results in altered transcriptional activation activity (Morse et al., 2009).

In this study, we screened for lignin biosynthesis-associated transcription factors (LTFs) by identifying proteins binding to the promoter of 4-coumarate-coenzyme A ligase (*4CL*), a key lignin biosynthetic gene in *Populus*. We identified *Populus* LTF1, which acts as a sensory switch for repression or activation of lignin biosynthesis based on its phosphorylation status in wood cells.

RESULTS

Identification of *LTF1* as a Regulator of Lignin Biosynthesis in Developing Xylem Cells

4CL is a key enzyme controlling metabolic flux through the lignin biosynthetic pathway (Lee et al., 1997; Hu et al., 1999; Gui et al., 2011). To elucidate how lignin biosynthesis is regulated in wood cells, we screened for transcription factors that bind the *4CL* promoter using yeast one-hybrid assays. From screening a *Populus* developing xylem expression library, we identified 20 transcription factors (Supplemental Table 1) that were potential LTFs. Among them, LTF1, LTF3, and LTF6 belong to MYB transcription factor gene family (LTF1: Potri.004G174400; LTF3: Potri.003G114100; LTF6: Potri.017G130300 in the Phytozome database, https://phytozome.jgi.doe.gov/pz/portal.html), and LTF1 was selected for further characterization because it was predominantly expressed in developing xylem (Supplemental Figure 1), a main location for lignin biosynthesis.

We generated and purified recombinant LTF1 protein using an *Escherichia coli* expression system (Invitrogen). Binding of LTF1 to the *4CL* promoter was verified by electrophoretic mobility shift assay (EMSA) and a yeast one-hybrid assay (Supplemental Figure 2A–2C). Subcellular localization analysis showed that LTF1-mCherry and DAPI were co-localized in the nucleus in tobacco epidermal cells (Supplemental Figure 2D). Transcriptional activation analysis in yeast indicated that LTF1 possesses transcriptional repression activity (Supplemental Figure 2E and 2F). Because there are two *LTF1* homologs (*LTF1-h*) (Potri.009G134000 and Potri.005G112000 named *LTF1-h1* and *LTF1-h2*, respectively) in the *Populus* genome (Supplemental Figure 3), expression of which partially overlaps with that of *LTF1* (Supplemental Figure 1), *LTF1* function was examined in greater detail using a CRISPR/Cas9 genome-editing system (Supplemental Figure 4A and 4B). We generated a series of single- and double-knockout *Populus* mutants of the *LTF1* homologous genes in order to ascertain the genetic function of *LTF1*. As shown in Supplemental Figure 4C, the mutants used in functional characterization included the following *LTF1* edited *Populus* lines (LE): (1) LE3, which is homozygous for a 1-bp insertion in *LTF* and heterozygous for mutations in both *LTF1-h1* and *LTF1-h2*; (2) LE56, which is homozygous for mutations in *LTF1* and *LTF1-h2*; (3) LE23, which is homozygous for mutations in *LTF1-h1* and *LTF1-h2*; and (4) LE32, a homozygous *LTF1-h2* mutant. LE62, without mutations, was used as a control (Supplemental Figure 4C).

The independent mutant lines were clonally propagated through cutting to produce at least eight copies of each line to serve as biological replicates. The growth behavior and phenotypes of these lines were examined. Compared with the unedited line (LE62), *LTF1* mutants (LE3 and LE56) had shorter stems and internodes (Figure 1A–1C). Moreover, *LTF1* mutant LE56 had a smaller stem diameter (Figure 1D). In developing xylem tissue, both *LTF1* mutants (LE3 and LE56) showed higher lignification and a wider lignified xylem region than the control and the lines without mutations in *LTF1* (LE23 and LE32) (Figure 1B). The *LTF1* knockout mutants had about 20% higher lignin content (Figure 1F) but did not show significant differences in crystalline cellulose and xylose content (Figure 1G and 1H). Consistent with this, expression of the key lignin biosynthesis genes (*PAL2*, *C4H1*, *C3H2*, *4CL1*, *CAld5H*, *COMT2*, and *CCoAOMT1*) (Osakabe et al., 1999; Boerjan et al., 2003) was significantly higher in the *LTF1* mutants than in the control, while the transcript levels of genes associated with cellulose biosynthesis (*CESA4*, *CESA7*, and *CESA8*) or hemicellulose biosynthesis (*GT43* and *GT8D*) did not show significant differences (Figure 1I). EMSA analysis also revealed that LTF1 was able to bind the promoters of the lignin biosynthesis genes *COMT2* and *CCoAOMT1* (Supplemental Figure 5). It is likely that *LTF1* is specifically involved in repressing lignin biosynthesis during xylem development.

LTF1 Protein Level Affects Lignification in Developing Xylem Cells

To detail how *LTF1* regulates lignin biosynthesis, we generated transgenic plants overexpressing *LTF1* (*LTF1OE*). Thirty-six independent transgenic lines were generated and displayed modified growth morphology and lignin deposition. The transgenics could be classified into three types based on the severity of their growth phenotypes. Three representative *LTF1*-overexpression (LO) transgenic lines, LO7 (type 1, 27/36), LO11 (type 2, 7/36), and LO23 (type 3, 2/36) were selected for more detailed characterization. The transgenics were grown in a phytotron for the first 2 months and were then moved to a glasshouse to grow. At 2 months old in the phytotron, the morphology of LO7 was

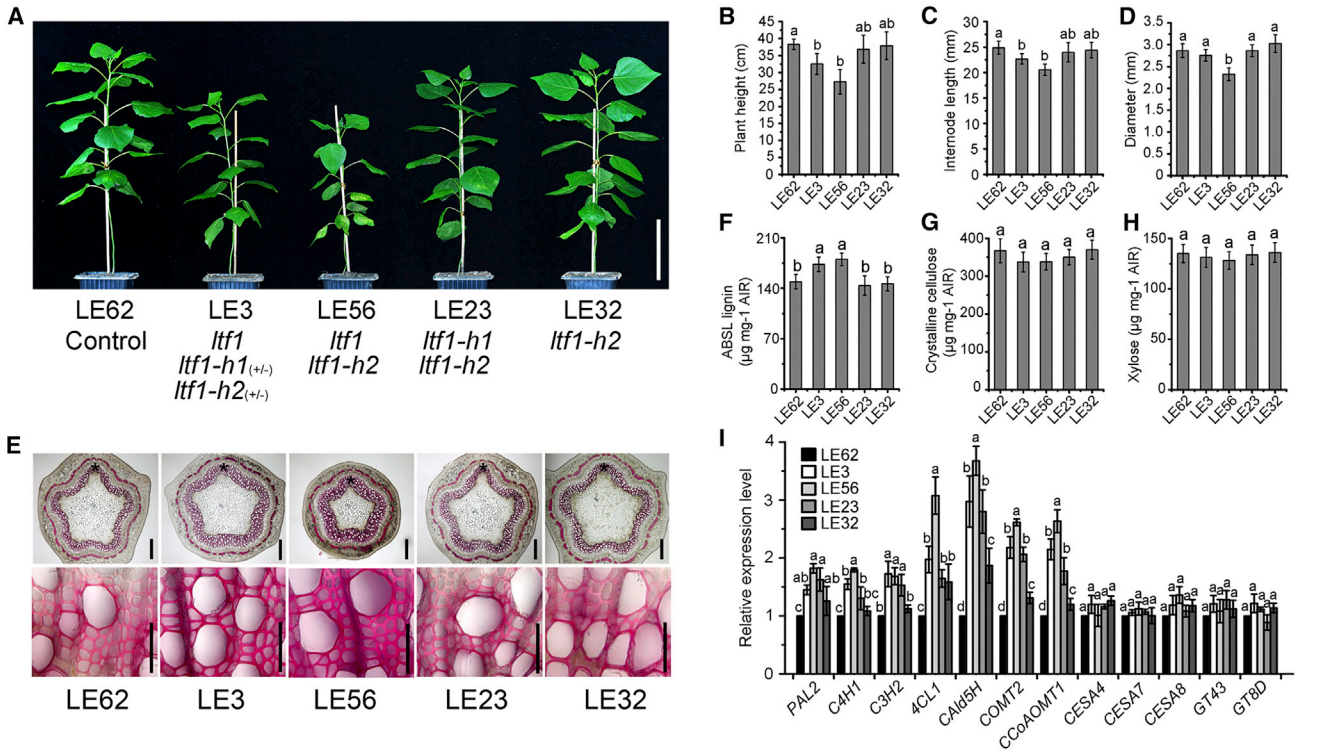

Figure 1. Knockout of *LTF1* Increased Lignin Deposition in Developing Xylem of *Populus*.

(A) Morphology of plants with mutations in *Populus LTF1* and its homologs (*LTF1-h1* and *LTF1-h2*) at 2 months old. Mutants were generated through CRISPR/Cas9 genome editing. +/−, heterozygous mutant; −, mutated; +, not mutated. Scale bar, 10 cm.

(B–D) Plant height **(B)**, internode length **(C)**, and stem diameter **(D)** in the mutants at the 2-month-old stage. Plant height and diameter: means ± SE of eight clonally propagated plants; Internode length: means ± SE of 80 internodes from eight plants.

(E) Images of cross-sections of the 11th internode stained with phloroglucinol–HCl (upper panel). Scale bar, 500 μm. Images in the lower panel are close-up images of the lignified xylem cells indicated by an asterisk in the upper panel. Scale bar, 50 μm.

(F–H) Lignin content, crystalline cellulose content, and xylose content in the stems of the 2-month-old plants. Results are means ± SE of three replicate determinations. ABSL, acetyl bromide-soluble lignin.

(I) Expression of genes involved in secondary cell-wall biosynthesis. Gene expression in the top three internodes of the 2-month-old plants was determined using qRT–PCR analysis. Results are means ± SE of three biological repeats.In **(B)** to **(D)** and **(F)** to **(I)**, different lowercase letters indicate significant differences at $p < 0.01$ by ANOVA.

similar to that of the control, while LO11 exhibited uneven leaf blades and soft stems. LO23 showed dwarfism, dark-green leaves, uneven leaf blades, distorted leaf veins, and soft stems (Figure 2A). The level of *LTF1* transcript was different in the three transgenic lines (Figure 2G) and was related to the severity of the growth phenotypes including changes in plant height, internode length, and stem diameter (Figure 2A and 2D; Supplemental Figure 6A and 6B). In xylem tissue, cell walls in LO11 and LO23 had less lignin deposition, but there was no apparent change in LO7 (Figure 2C). Consistent with this, lignin content was 13% lower in LO11 and 30% lower in LO23 than in the control (Figure 2F). The crystalline cellulose and xylose levels were not changed in the transgenics (Supplemental Figure 6E and 6F). When the transgenics were grown in a glasshouse to 8 months old, the severity of the transgenic growth phenotypes (such as plant height and lignin deposition) diminished (Figure 2B and Supplemental Figure 6C–6F). However, the level of *LTF1* transcripts was the same as that of the 2-month-old plants in the phytotron (Figure 2G). We then examined the abundance of LTF1 protein in the transgenics. The LTF1 protein abundance in LO7, LO11, and LO23 was significantly different at 2 months but this difference diminished by 8 months (Figure 2H). The abundance of LTF1 protein was substantially lower in the 8-month-old transgenics (Figure 2H). The abundance of LTF1 protein was related to the growth performance observed in the *LTF1OE* transgenics, suggesting that the abundance of the LTF1 protein, rather than the level of *LTF1* transcript, more significantly affected the phenotype.

LTF1 Is Phosphorylated at Thr146 and Thr178

To investigate the cause of the change in LTF1 protein level, we looked at potential post-translational modifications of LTF1. First, we isolated LTF1 proteins from transgenic lines expressing *LTF1-3FLAG* grown in the phytotron or glasshouse. Proteins were concentrated and immunoprecipitated using anti-FLAG agarose beads, and the precipitated proteins were analyzed using liquid chromatography–tandem mass spectrometry (LC–MS/MS). In extracts from 8-month-old plants grown in the glasshouse, phosphorylation of LTF1 was detected at two sites (Thr146 and Thr178) within the peptides GIDPATHRPLNEPAQEASTTISFSTT(pT)PAK and EEK(pT)PVQER(Supplemental Figure 7A and 7B). Phosphorylation at these sites was not detected in the extracts from 2-month-old transgenics grown in

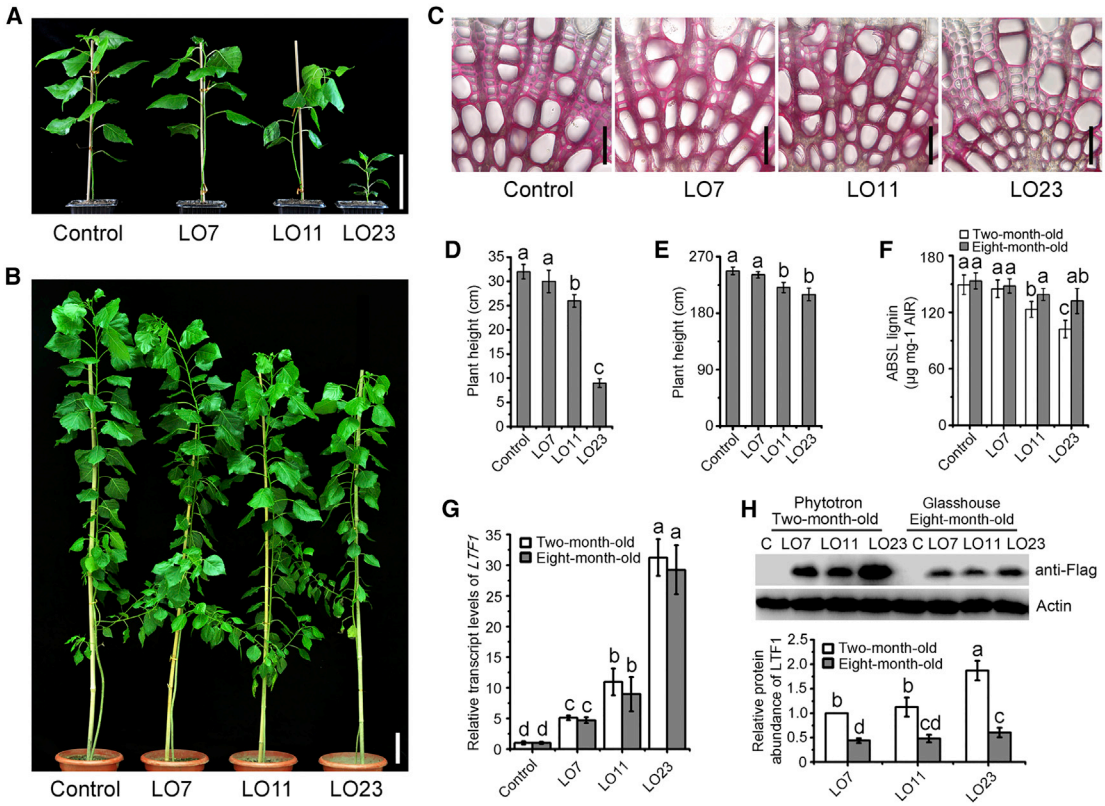

Figure 2. LTF1 Protein Levels Affected Secondary Cell-Wall Lignification in *Populus*.

(A and B) Transgenic *Populus* overexpressing *LTF1* at 2 months old (grown in a phytotron) **(A)** and at 8 months old (grown in a glasshouse) **(B)**. Scale bar, 10 cm.

(C) Cross-sections (11th internode) of the control and different *LTF1*-overexpressing (*LTF1OE*) lines stained with phloroglucinol–HCl to visualize total lignin. Scale bar, 50 μm.

(D and E) Plant height of *LTF1OE* transgenics at the 2-month (D) and 8-month **(E)** stages. Plant height: means ± SE of eight clonally propagated plants.

(F) Lignin content in the stems of the 2-month-old and 8-month-old plants. The stems at the same internodes in the shoot tips of the 2-month-old and 8-month-old plants were collected for lignin content determination. Results are means ± SE of three replicate determinations. ABSL. acetyl bromide-soluble lignin.

(G) *LTF1* transcript levels in control and *LTF1OE* transgenic lines at the 2-month and 8-month stages. Results are means ± SE of three biological repeats.

(H) Protein abundance of LTF1 in *LTF1OE* transgenic *Populus* at the 2-month and 8-month stages was examined by immunoblotting assay (upper panel). The signal density of the immunoblotted LTF1 was quantified based on the three biological replicates (lower panel). The relative protein abundance in the 2-month-old *LTF1OE* line LO7 was set as 1.

In **(D)** to **(H)**, different lowercase letters indicate significant difference at $p < 0.01$ by ANOVA.

the phytotron. We speculate that different environmental stimuli in the phytotron and the glasshouse likely contributed to differential LTF1 phosphorylation.

Mutating LTF1 at Specific Sites Results in Persistent Suppression of Lignification in Developing Xylem Cells

To determine whether and how LTF1 phosphorylation plays a role in *Populus*, we introduced mutations at the sites of phosphorylation (Thr146 and Thr178) to produce phosphorylation-null LTF1 ($LTF1^{T146/178A}$, designated as $LTF1^{AA}$). We generated transgenic *Populus* plants expressing $LTF1^{AA}$ (*35S:LTF1*^{AA}*-3FLAG*, designated as $LTF1^{AA}$*OE*). Fifty-five independent $LTF1^{AA}$-mutation (LM) transgenic lines were produced, which showed varying degrees of dwarfism, dark-green uneven leaf blades, distorted leaf veins, soft stems, pendant growth, increased branch number, and reduced root growth over the 8-month growth period (Figure 3A and 3B; Supplemental Figure 8). Compared with the control plants, the transgenics exhibited severe morphological changes. As shown in Figure 3C–3E, the transgenics displayed a 45%–75% decrease in height, 23%–50% decrease in stem diameter, and 26%–60% decrease in internode length. Lignin deposition was significantly reduced in the fiber cells of the transgenics (Figure 3F). Distorted or collapsed xylem vessels were observed (Figure 3F), and the content of lignin, crystalline cellulose, and xylose was reduced (Figure 3G–3I).

In the $LTF1^{AA}$*OE* transgenics, the *LTF1* transcript levels were 4- to 10-fold higher than in the control (Figure 3J). The severity of the phenotypic changes and reduction in lignin content correlated with the $LTF1^{AA}$ transcript levels at both the 2-month and 8-month stages (Figure 3A, 3B, 3J, and 3K). We also compared the *LTF1* transcript levels in the *LTF1OE* and $LTF1^{AA}$*OE* transgenics at the 8-month stage. The *LTF1* transcript level was

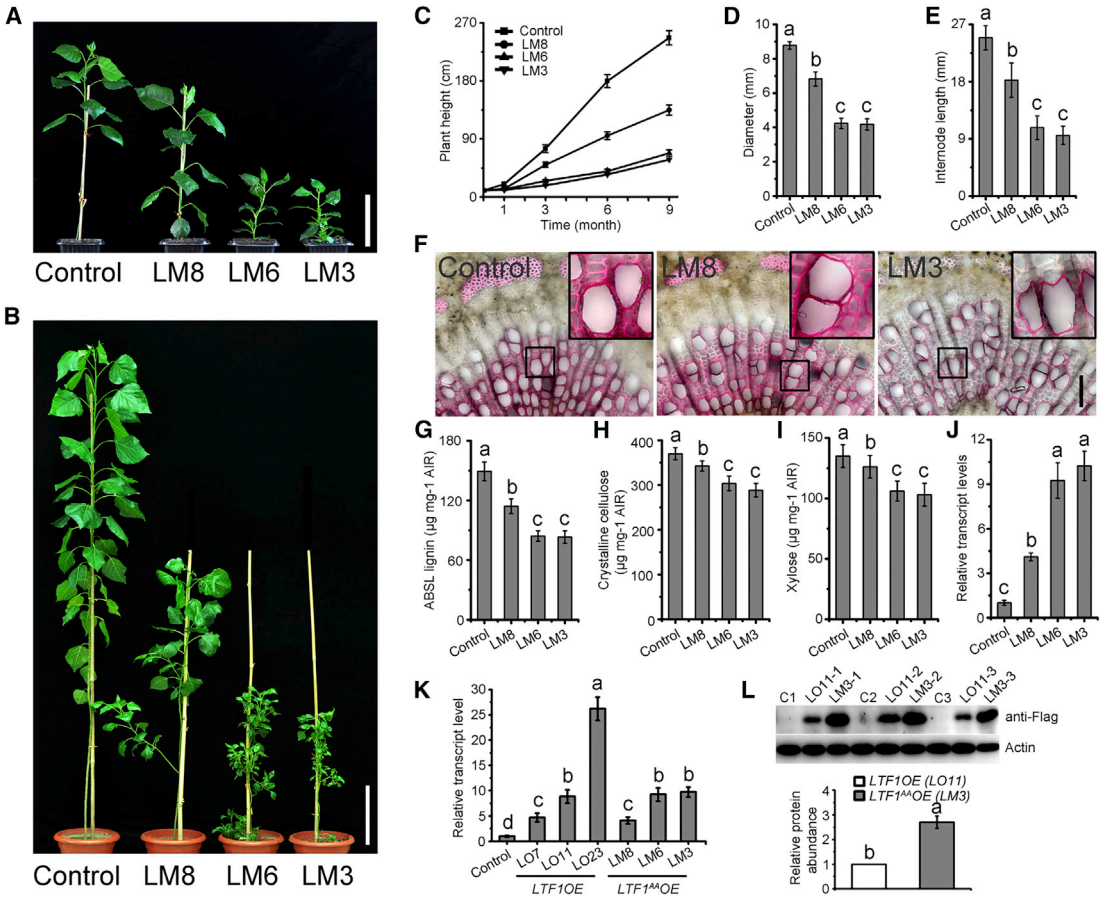

Figure 3. Expression of *LTF1^{AA}* Suppressed Lignin Deposition in Developing Xylem of *Populus*.

(A and B) Phenotypes of the *LTF1^{AA}*-overexpressing (*LTF1^{AA}OE*) plants grown in a phytotron at the 2-month stage **(A)** and grown in a glasshouse at the 8-month stage **(B)**.

(C–E) Plant height **(C)**, diameter **(D)**, and internode length **(E)** of the transgenics and control plants. Plant heights were measured at 1, 3, 6, and 9 months. The diameter and internode length were measured at 8 months. Plant height and diameter: means ± SE of six clonally propagated plants; internode length: means ± SE of 60 internodes from six plants.

(F) Cross-sections (11th internode) of the control and *LTF1^{AA}OE* lines stained with phloroglucinol–HCl. Inset: enlarged image of the developing xylem vessels and fibers. Scale bar, 100 μm.

(G–I) Content of lignin **(G)**, crystalline cellulose **(H)**, and xylose **(I)** in the xylem tissue of the 2-month-old plants. Results are means ± SE of three replicate determinations. ABSL, acetyl bromide-soluble lignin.

(J) *LTF1* transcript levels in the control and *LTF1^{AA}OE* transgenics at the 2-month stage. Results are means ± SE of three biological repeats.

(K) Comparison of *LTF1* transcript level in the *LTF1OE* and *LTF1^{AA}OE* transgenics at the 8-month stage. Results are means ± SE of three biological repeats.

(L) *LTF1* protein abundance in the *LTF1OE* and *LTF1^{AA}OE* transgenics. Three clonally propagated copies at the 8-month stage were used for the immunoblotting assay (upper panel). Signal density was quantified based on three biological repeats (lower panel).

In **(D)**, **(E)**, and **(G)** to **(L)**, different lowercase letters indicate significant difference at $p < 0.01$ by ANOVA.

similar in the *LTF1OE* transgenic line LO11 and the *LTF1^{AA}OE* transgenic line LM3 (Figure 3K). However, the growth phenotypes of the two types of transgenics appeared strikingly different (Figures 2B and 3B). This prompted us to examine whether LTF1 protein abundance caused the growth differences between the two types of transgenics. The *LTF1^{AA}OE* transgenics (clonal propagates of LM3: LM3-1, and LM3-2, and LM3-3) accumulated a much higher level of LTF1 protein than the *LTF1OE* transgenics (clonal propagates of LO11: LO11-1, LO11-2, and LO11-3) (Figure 3L). Mutation of the LTF1 phosphorylation sites Thr146 and Thr178 resulted in higher LTF1 protein abundance.

When we examined expression of lignin biosynthesis genes (*PAL2*, *C4H1*, *C3H2*, *4CL1*, *CAld5H*, *COMT2*, and *CCoAOMT1*) in transgenic plants transformed with the two different *LTF1* constructs (*LTF1^{AA}* and *LTF1*), we found that the expression of these genes was suppressed in both the *LTF1^{AA}OE* (LM3) and *LTF1OE* (LO11) transgenics (Supplemental Figure 9). However, the suppression was significantly stronger in *LTF1^{AA}OE* than in *LTF1OE* (Supplemental Figure 9).

Phosphorylation of LTF1 Affects Its Stability

To further elucidate the reason for the difference in LTF1 level in the *LTF1^{AA}OE* and *LTF1OE* transgenics, we generated

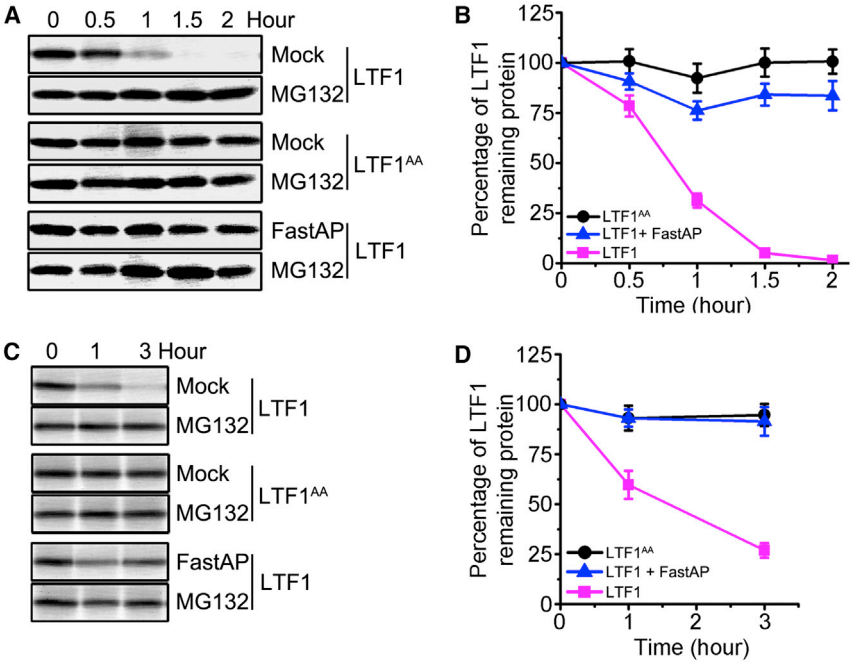

Figure 4. Mutation of LTF1 Phosphorylation Sites Inhibited LTF1 Degradation.

(A and B) Recombinant proteins of LTF1 and LTF1^{AA} were expressed and purified from *Escherichia coli*. Recombinant proteins were incubated with or without 5 μM MG132 (a proteasome inhibitor) or 10 U of FastAP (a thermosensitive alkaline phosphatase) at 37°C in cell lysate from the developing xylem of *Populus* grown in a glasshouse at the 8-month-old stage. LTF1 and LTF1^{AA} accumulation was examined by immunoblotting assay **(A)** and quantified based on the signal density from three replicates **(B)**.

(C and D) Cell lysate isolated from *LTF1* or *LTF1^{AA}* transgenics was incubated with or without MG132/FastAP at 37°C for different times. LTF1 and LTF1^{AA} accumulation was examined by immunoblotting assay **(C)** and protein abundance was quantified based on the signal density from three replicates **(D)**.

recombinant LTF1 and LTF1^{AA} proteins in *E. coli* and examined their stability in cell lysates isolated from developing xylem of *Populus* grown in a glasshouse. LTF1 was rapidly degraded in total cell lysate, and this degradation was inhibited by the proteasome inhibitor MG132 (Figure 4A and 4B). However, the mutated LTF1^{AA} protein was not degraded (Figure 4A and 4B). When alkaline phosphatase (FastAP) was added to the assay system, LTF1 degradation was inhibited, indicating that LTF1 degradation is dependent on its phosphorylation (Figure 4A and 4B). Furthermore, when plant-produced LTF1 and LTF1^{AA} were used in the degradation analysis, LTF1^{AA} was highly stable while LTF1 was readily degraded (Figure 4C and 4D). Thus, phosphorylation regulates the stability of LTF1 in a manner related to proteasome degradation.

LTF1 Is Phosphorylated by MPK6 through Direct Interaction

Next, we performed a yeast two-hybrid assay and immunoprecipitation followed by liquid chromatography–tandem mass spectrometry (IP–MS) analysis to search for possible kinases that catalyze LTF1 phosphorylation. The LTF1 C-terminal region (amino acid residues 151–268) which contains an ethylene response factor-associated amphiphilic repression motif, was used as bait to screen a cDNA library derived from *Populus* developing xylem. A MAPK candidate (encoded by Potri.007G139800) was identified. Sequence analysis indicated that this protein is homologous to *Arabidopsis* MPK6 and named PdMPK6 (Supplemental Figure 10). We employed LTF1^{AA}-3FLAG transgenic plants to identify LTF1-interacting proteins through IP–MS analysis because LTF1 was readily degraded in the xylem cell protein extracts (Figure 4). PdMPK6 (Potri.007G139800) was among the LTF1-interacting proteins identified (Supplemental Table 2), thus confirming the interaction between LTF1 and PdMPK6.

The direct interaction between LTF1 and PdMPK6 was further verified using a yeast two-hybrid assay, bimolecular fluorescence complementation (BiFC) assay, and co-immunoprecipitation (Co-IP). In yeast, the interaction between LTF1 and PdMPK6 and between LTF1 and the constitutively active form of MPK6 (PdMPK6-CA) was detected, but no interaction was detected between pGADT7 and PdMPK6/PdMPK6-CA, or between LTF1 and pGBKT7 (Figure 5A). A BiFC assay was performed in a tobacco expression system to verify the interaction of the two proteins. A strong fluorescent signal was detected in the nucleus of tobacco leaf epidermal cells that co-expressed LTF1 tagged with the C-terminal half of yellow fluorescent protein (YFP) (LTF1-YC) and PdMPK6 fused with the N-terminal half of YFP (PdMPK6-YN) (Figure 5B). No fluorescence signal was detected with co-expression of LTF1-YC and -YN, or co-expression of PdMPK6-YN and -YC (Figure 5B). In addition, the interaction was verified through coIP analysis. LTF1-Myc and PdMPK6-FLAG co-expressed in tobacco leaves were able to be co-immunoprecipitated (Figure 5C).

We then examined whether PdMPK6 can phosphorylate LTF1. We generated recombinant His-tagged LTF1, PdMPK6, and PdMKK4^{DD} (T218D and S224D, a constitutively active form of MKK4 [Asai et al., 2002]) in *E. coli* for a phosphorylation assay. LTF1 was phosphorylated by PdMPK6 after activation by PdMKK4^{DD} (Figure 5D). In contrast, LTF1 was not phosphorylated by PdMPK6 in the absence of MKK4^{DD} (Figure 5D). When the Thr146 and Thr178 residues in LTF1 were mutated to alanine, the phosphorylation signal was drastically reduced (Figure 5D). The specific phosphorylation sites were examined by LC–MS/MS. Phosphorylation at Thr146 and Thr178 was detected in LTF1 that was incubated with PdMPK6/PdMKK4^{DD} (Supplemental Figure 11A and 11B), but not detected in the absence of PdMPK6/PdMKK4^{DD} (Supplemental Figure 11C and 11D). These results confirmed that PdMPK6 indeed phosphorylates LTF1 at the sites Thr146 and Thr178.

Next, we examined whether LTF1 phosphorylation status is related to PdMPK6 *in planta*. First, LTF1 phosphorylation was

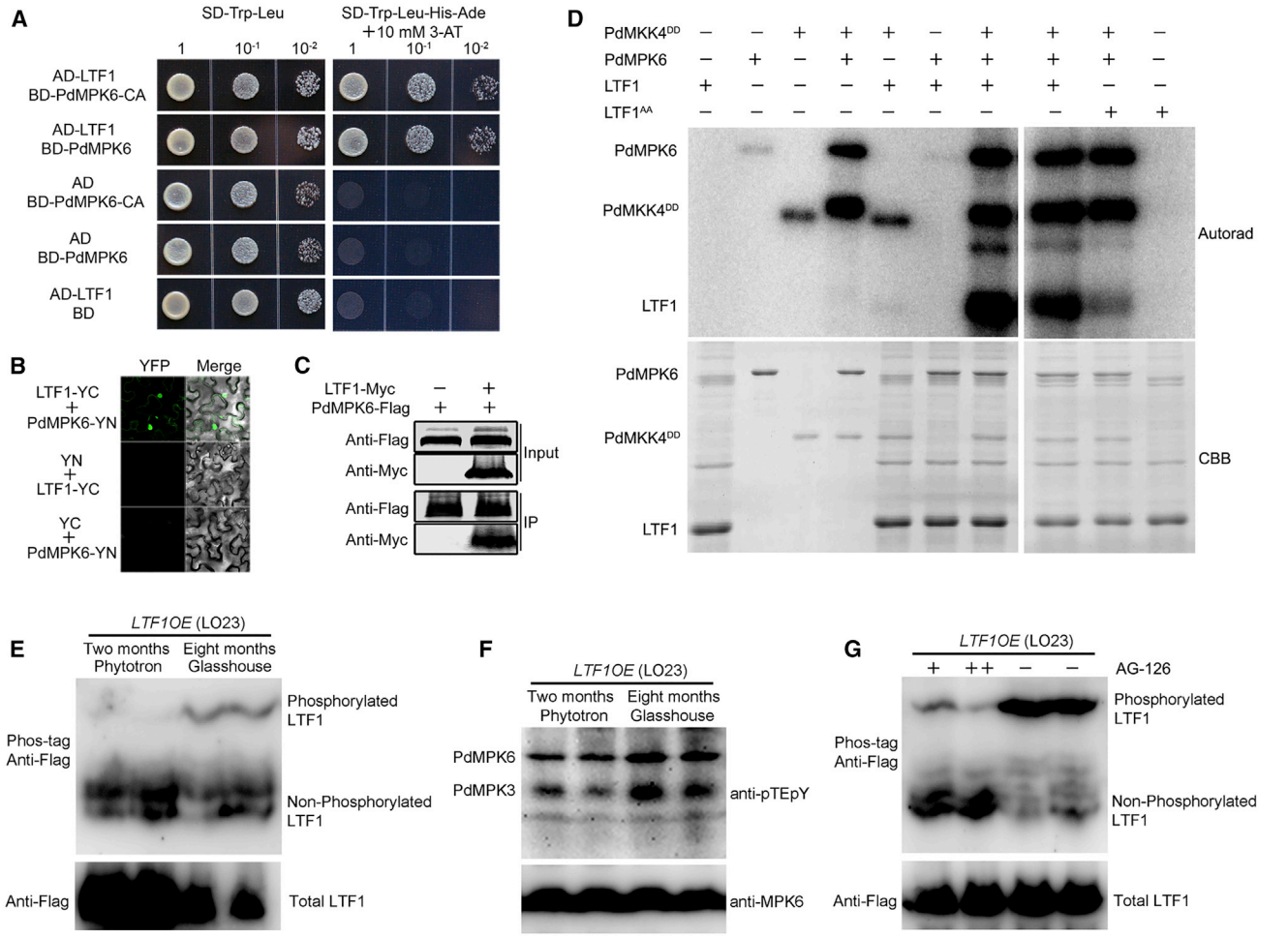

Figure 5. PdMPK6 Directly Interacted with and Phosphorylated LTF1 both *In Vitro* and *In Vivo*.

(A–C) Interaction between LTF1 and PdMPK6 was confirmed by yeast two-hybrid **(A)**, BiFC **(B)**, and Co-IP **(C)** analyses.

(D) LTF1, LTF1^{AA}, PdMPK6, and PdMKK4^{DD} (a constitutively active form of PdMKK4) were expressed in *E. coli* and purified for *in vitro* phosphorylation assays. LTF1 or LTF1^{AA} was incubated with or without PdMPK6/PdMKK4^{DD} at 30°C for 1 h. After separation on an SDS–PAGE gel, images were obtained using a phosphor imager (upper panel). The gel was stained with Coomassie brilliant blue R250 (lower panel). Autorad, autoradiograph; CBB, Coomassie brilliant blue staining.

(E) LTF1 phosphorylation was examined in an *LTF1-OE* transgenic line (#23) at the 2-month and 8-month stages by Phos-tag gel electrophoresis and immunoblotting assays (upper panel). The LTF1 protein was examined by immunoblotting analysis using antibodies against FLAG (lower panel). Lower levels of LTF1 proteins with higher levels of phosphorylation were detected in 8-month-old plants.

(F) PdMPK6 phosphorylation was detected by immunoblotting analysis using anti-pTEpY and anti-MPK6 antibodies. PdMPK6 displayed higher levels of phosphorylation in 8-month-old plants than in the 2-month-old plants.

(G) LTF1 phosphorylation in the *LTF1-OE* transgenic line LO23 at the 8-month stage was inhibited by AG-126 (an MPK6 inhibitor). Phos-tag (upper panel) and LTF1 (lower panel) immunoblots are shown (+: 50, ++: 100, −: 0 μM AG-126).

examined in *LTF1OE* plants grown in a phytotron (2 months old) and in a glasshouse (8 months old) using a Phos-tag immunoblot assay. LTF1 displayed a high level of phosphorylation in plants grown in the glasshouse but low levels in those from the phytotron (Figure 5E). Consistent with the higher level of LTF1 phosphorylation, a higher level of the active form of PdMPK6 along with PdMPK3 was detected in the plants grown in the glasshouse than in those grown in the phytotron (Figure 5F). Second, a specific MPK6 inhibitor, AG-126 (Hanisch et al., 2001), was used to test whether LTF1 phosphorylation is dependent on MPK6 activity. When AG-126 was applied to the plants, LTF1 phosphorylation was significantly impeded (Figure 5G). Together, these results demonstrated that LTF1 is phosphorylated at Thr146 and Thr178 by active PdMPK6.

LTF1 Phosphorylation Activates Lignin Deposition

Lignin biosynthesis can be induced by environmental stimuli, such as mechanical wounding. We examined whether such induction is mediated through LTF1 phosphorylation. We observed induced lignin deposition after mechanical wounding in wild-type (WT) and *LTF1OE* plants (Figure 6A and 6B). However, this induction was not observed in *LTF1^{AA}OE* plants (Figure 6C). Expression of the key lignin biosynthesis genes was significantly induced by mechanical wounding in *LTF1OE* and

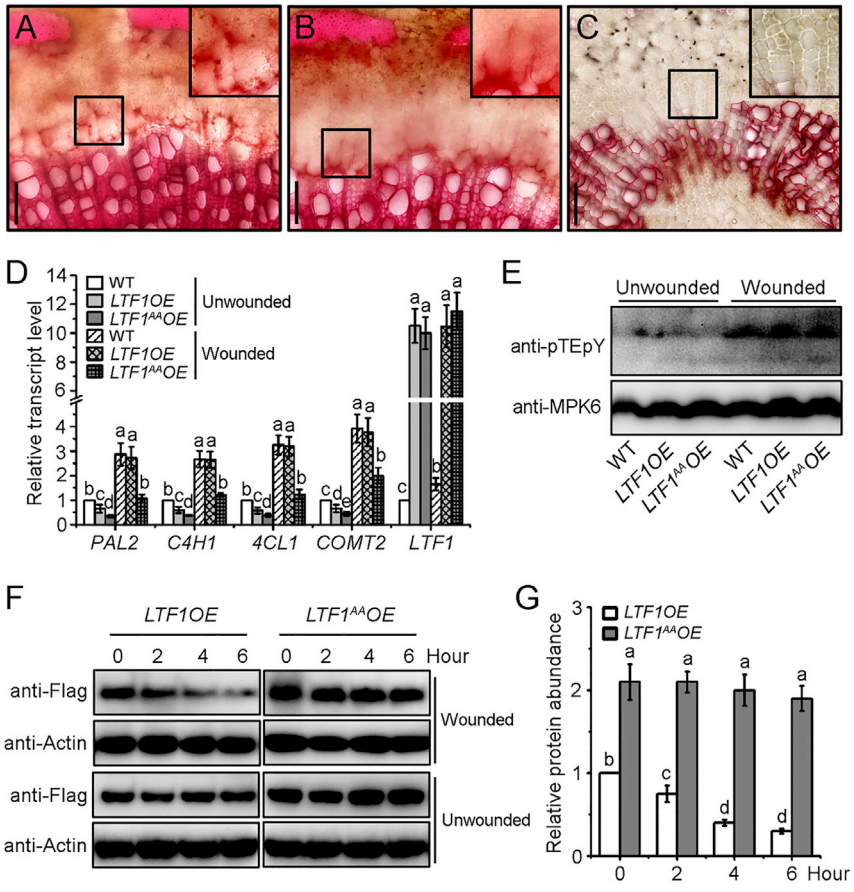

Figure 6. Wounding Activated PdMPK6 and Promoted LTF1 Degradation.

(A–C) WT **(A)**, *LTF1OE* **(B)**, and *LTF1^{AA}OE* **(C)** plants were wounded at the 15th internode. Four days after wounding, lignin deposition was examined in the cross-sections next to the wounded sites by phloroglucinol–HCl staining. Inset: enlarged image of the cells in the area bound by the square. Scale bar, 100 μm.

(D) Expression of lignin biosynthesis genes was examined in WT, *LTF1OE*, and *LTF1^{AA}OE* plants after 2 h with or without wounding. Results are means ± SE of three biological repeats.

(E) PdMPK6 phosphorylation after wounding was detected by immunoblotting analysis using anti-pTEpY (upper panel) and anti-MPK6 (lower panel) antibodies.

(F and G) LTF1 and LTF1^{AA} were examined in transgenics at different times after wounding or not wounding. Total proteins were extracted, and an immunoblotting assay was performed using antibodies against FLAG and actin **(F)**. Abundance of LTF1 or LTF1^{AA} was quantified based on the signal density from three replicates **(G)**. The relative protein abundance in *LTF1OE* at 0 h (before wounding) was set as 1. LTF1 degradation is induced by wounding.

In **(D)** and **(G)**, different lowercase letters indicate significant difference at $p < 0.01$ by ANOVA.

WT plants, and mildly induced in *LTF1^{AA}OE* plants (Figure 6D). Moreover, expression of these genes was significantly higher in *LTF1OE* and WT plants than that in *LTF1^{AA}OE* after wounding (Figure 6D). The active form of PdMPK6 was detected at 15 min after wounding in WT, *LTF1OE*, and *LTF1^{AA}OE* plants (Figure 6E). Consistent with the increase in the active form of PdMPK6, LTF1 abundance was reduced within 2 h after wounding in the *LTF1OE* plants but not changed in the *LTF1^{AA}OE* plants and unwounded plants (Figure 6F and 6G). These results suggest that LTF1 is phosphorylated by the active form of PdMPK6, which is activated by mechanical wounding, and that phosphorylated LTF1 undergoes degradation, thereby activating lignin biosynthesis (Figure 7).

DISCUSSION

LTF1 Modulates Lignin Biosynthesis in *Populus* by Binding the Promoters of Key Lignin Biosynthetic Genes

In trees, lignin biosynthesis in secondary xylem is regulated by a multilayered transcriptional regulatory network (Ye and Zhong, 2015). *LTF1* encodes an MYB transcription factor. A group of 192 MYB transcription factors has been identified in the genome of *Populus* (Wilkins et al., 2009), but their genetic functions have largely not been demonstrated. *LTF1* shares a high degree of sequence similarity with *AtMYB4*, *AtMYB7*, and *AtMYB32* from the herbaceous plant *Arabidopsis*. *AtMYB4* is involved in the regulation of phenylpropanoid metabolism, and its expression is regulated by different environmental conditions such as wounding and UVB light (Jin et al., 2000). In switchgrass, ectopic overexpression of *PvMYB4*, an *AtMYB4* homolog, resulted in alterations in phenylpropanoid metabolism and lignin content (Shen et al., 2012). The homologs of MYB4 from snapdragon (Tamagnone et al., 1998), maize (Sonbol et al., 2009; Fornale et al., 2010), and eucalyptus (Legay et al., 2010) have been suggested to play a role in the regulation of lignin deposition, but the mechanisms underlying *MYB* regulation of this process have not yet been elucidated. As illustrated in Figure 7, we ascertained that the transcription factor LTF1 binds to the promoters of key lignin biosynthesis genes such as *4CL* to repress lignin biosynthesis. 4CL catalyzes a key step in monolignol biosynthesis pathways and its regulation has critical effects on lignin deposition (Lee et al., 1997; Hu et al., 1999; Gui et al., 2011). Our results from observations of *LTF1* knockout mutants generated through CRISPR/Cas9 editing and *LTF1*-overexpression lines, demonstrated that *LTF1* plays a crucial role in the control of lignin biosynthesis in *Populus*.

Dynamic Regulation of Lignin Biosynthesis in Wood Cells through LTF1 Phosphorylation

LTF1 function is dependent on its phosphorylation status, which determines its stability and affects its activity *in planta*. We determined that phosphorylated LTF1 can be degraded via the proteasome pathway; however, a phosphorylation-null LTF1 protein, which cannot be phosphorylated at the Thr146 and Thr178 sites, is resistant to degradation. The finding that LTF1 phosphorylation plays a role in regulating lignin biosynthesis reveals a new mechanism by which lignin biosynthesis can be regulated in a dynamic

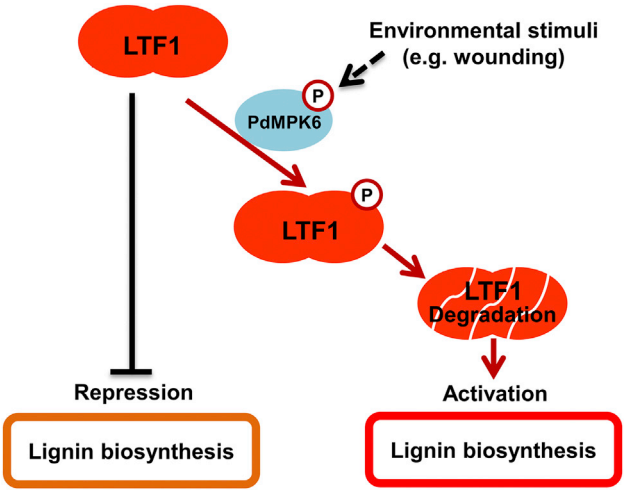

Figure 7. A Proposed Model for the Role of LTF1 Phosphorylation Mediated by PdMPK6 in the Regulation of Lignin Biosynthesis.

LTF1 directly binds to the promoters of key lignin biosynthesis genes to repress lignin biosynthesis. PdMPK6, which is activated by environmental stimuli such as wounding, can phosphorylate LTF1. LTF1 phosphorylation results in its degradation and the release of LTF1 repression of lignin biosynthesis.

manner in response to various stimuli. Based on the evidence presented, we postulate a model (Figure 7) in which LTF1 acts as a sensor that in response to environmental stimuli can switch on or off lignin biosynthesis during plant growth and adaptation. The involvement of MAPKs in the phosphorylation of MYB transcription factors has been reported in *Arabidopsis* and loblolly pine (Morse et al., 2009; Persak and Pitzschke, 2013; Li et al., 2016). For example, AtMYB75 is phosphorylated by MPK4 and is required for light-induced anthocyanin accumulation in *Arabidopsis* (Li et al., 2016). In loblolly pine, PtMYB4 (a homolog of AtMYB46, Supplemental Figure 3) is phosphorylated by MPK6 during xylem development (Morse et al., 2009). However, it is unclear how phosphorylation affects the functions of these proteins. In this study, PdMPK6 was shown to be an LTF1-interacting protein. Activation of PdMPK6 in response to wounding promoted LTF1 phosphorylation in wood cells. When activated, PdMPK6 is able to catalyze the phosphorylation of LTF1 at Thr146 and Thr178, which leads to LTF1 degradation and release of LTF1 repression of lignin biosynthesis.

It is believed that the MPK6 signaling module can be activated by various biotic and abiotic environmental stimuli such as cold, light, and drought (Colcombet and Hirt, 2008; Li et al., 2016, 2017; Zhao et al., 2017). It appears that the signaling specificity of the MAPK cascade is conferred by the ability of MAPKs to phosphorylate different substrates with specific functions. Here LTF1 was characterized as a PdMPK6 substrate in the regulation of lignin biosynthesis. Usually, lignin biosynthesis is upregulated under various environmental stresses (Moura et al., 2010; Le Gall et al., 2015). Thus it would be very interesting to further investigate whether the enhancement of lignin biosynthesis under environmental stresses is generally achieved through the activation of the MPK cascade and LTF1 phosphorylation.

Potential Tools for Precise Regulation of Lignin Biosynthesis during Plant Growth

Precise control of lignin biosynthesis in specific cells is essential for higher plant growth and development (Boerjan et al., 2003; Fraser and Chapple, 2011; Wang et al., 2018). To ensure that lignin deposition occurs in specific cell types and at the right time, a network of factors have to work in concert to precisely regulate lignin biosynthesis throughout the course of plant growth (Kubo et al., 2005; Lee et al., 2013; Huang et al., 2018). In the herbaceous plant *Arabidopsis*, lignin biosynthesis is controlled by a multilayered transcriptional regulatory network (Zhong and Ye, 2007; Zhong et al., 2008; Zhou et al., 2009). For example, during root and inflorescence development in *Arabidopsis*, correct initiation of lignin biosynthesis is critical for normal growth (Kubo et al., 2005; Huang et al., 2018). In this study, *LTF1* was identified as a regulator modulating lignin biosynthesis in the developing xylem of *Populus*. At the protein level, LTF1 phosphorylation participates in the regulation of lignin biosynthesis in woody plants with evident effects on plant growth. Knockout of *LTF1* caused higher ligninification and abnormal growth phenotypes such as short stature. In contrast, plants overexpressing phosphorylation-null LTF1 displayed less ligninification and dwarfism. This reflects the importance of correct regulation of lignin biosynthesis for plant growth.

Being sessile, plants have evolved the ability to cope with environmental variation (Sultan, 2000). On the one hand, lignin can be employed as a defensive barrier, and its biosynthesis is regulated in response to environmental stress (Moura et al., 2010; Le Gall et al., 2015). On the other hand, lignin is recalcitrant toward lignocellulosic biomass processing, and modification of lignin biosynthesis has been of great interest for improving biomass utilization. As lignin biosynthesis and plant growth may be coregulated through a complex set of regulatory networks in a precise spatiotemporal manner (Xie et al., 2018), genetic engineering of lignin often incurs a growth penalty. The discovery of a sensory switch would aid in designing new tools to modify lignin biosynthesis. Such tools would be of particular interest for engineering lignin biosynthesis in concert with plant growth to better realize the immense potential of cellulosic biomass engineering for applications such as biofuel and fiber production.

METHODS

Plant Growth, Transgenic Plants, Gene Expression, and Phenotypic Analysis

Populus deltoides × *Populus euramericana* cv. "Nanlin895" was used in this study. For construction of the *LTF1*, *LTF1-h1*, and *LTF1-h2* CRISPR/Cas9 vectors, gene-specific target sequences were reassembled into *sgRNA* expression cassettes and then subcloned into a *pYLCRISPR/Cas9P35S-H* plasmid according to Ma et al. (2015). For WT *LTF1* and phosphorylation-null *LTF1* ($LTF1^{T146/178A}$, designated as $LTF1^{AA}$) overexpression, the full length coding sequences of *LTF1* and $LTF1^{AA}$ were digested with *Bam*HI and *Sal*I, and separately subcloned into a binary *pCAMBIA2300*:*35S-3FLAG* vector under the control of the 35S promoter. After the accuracy of the constructs was verified by sequencing, they were mobilized into *Agrobacterium tumefaciens* strain GV3101 for genetic transformation according to the protocol used in our laboratory (Li et al., 2003). Primers used in this study are provided in Supplemental Table 3. The WT and overexpression transgenic lines (*LTF1OE* and $LTF1^{AA}OE$) and *LTF1-Cas9* mutants were grown in a

phytotron under conditions of 60% relative humidity, a 12-h photoperiod, and 25°C constant temperature. Total RNA isolation and spatiotemporal analysis of gene expression, with or without wounding treatment, were performed as previously described (Gui et al., 2011). Total proteins were extracted from tissues, with or without wounding treatment, with 2× SDS–PAGE sample buffer (100 mM Tris–HCl [pH 6.8], 2% SDS, 100 mM dithiothreitol [DTT], 20% glycerol, 0.02% bromophenol blue) supplemented with 1× protease inhibitor cocktail (Roche) and 1× phosphatase inhibitor cocktail (Roche), and separated by SDS–PAGE (4% stacking gel and 10% separating gel). LTF1-3FLAG and $LTF1^{AA}$-3FLAG proteins were detected with an anti-FLAG antibody (Abmart). PdMPK6 protein was detected with an anti-pTEpY antibody (Cell Signaling Technologies) or anti-MPK6 antibody (Sigma).

For mechanical wounding analysis, stems at the 15th internode from 2-month old *Populus* were wounded with a razor blade. Four days after wounding, cross-sections next to the wounded sites were stained with phloroglucinol–HCl and observed under a microscope.

Plants were clonally propagated through cutting, and morphological parameters, including plant height, stem diameter, and internode length were measured in 2-month and/or 8-month-old trees. Plant height was determined as the shortest distance between the shoot tip and stem base; stem diameter was measured 50 cm above the stem base; internode length was measured from the 15th to 25th internode.

Histochemical Staining

Phloroglucinol–HCl staining was performed as previously described (Gui et al., 2011). Stems were hand sectioned and stained with 0.5% phloroglucinol (w/v) in 12% HCl and observed with a microscope (Olympus BX53) under white or UV light. Toluidine blue staining of paraffin-embedded tissue was performed as previously described (Gui et al., 2016).

Cell-Wall Composition Analysis

Stem tissue from 2-month-old and 8-month-old plants was collected and dried at 55°C. The dried shoot was ground to a fine powder by ball milling and used to prepare alcohol-insoluble residues according to Song et al. (2016). After starch was removed using 10 μl of amylase (50 μg/l ml H_2O, from *Bacillus* species; Sigma) and 5 μl of pullulanase (18.7 units, from *Bacillus acidopullulyticus*; Sigma), lignin, crystalline cellulose, and xylose contents were analyzed as previously described (Foster et al., 2010a, 2010b).

Electrophoretic Mobility Shift Assay

LTF1 coding sequences were amplified and cloned into the pET28a(+) vector (between *Nde*I and *Xho*I sites) and fused with a His6 tag at the C terminus (Novagen). LTF1-His protein was expressed in the *E. coli* BL21(DE3) strain (Invitrogen) and purified using nickel–nitrilotriacetic acid resin (Qiagen). Fragments of the Cy5-labeled *Pd4CL1*, *PAL2*, *C4H1*, *C3H2*, *CAld5H*, *COMT2*, and *CCoAOMT1* promoters and mutated *Pd4CL1* promoter were produced by PCR amplification using Cy5-labeled fluorescent primers or unlabeled competition primers. EMSA was performed as previously described (Gui et al., 2016).

Yeast One-Hybrid Assays

To examine LTF1 binding to the *Pd4CL1* promoter, we fused the coding sequence of *LTF1* in-frame with *GAL4-AD* to construct the *pPC86-LTF1* plasmid. The *Pd4CL1* promoter fragment (107–268 bp upstream of the initiation codon ATG) was inserted into the reporter construct *p178* to generate the P_{Pd4CL1}-*lacZ* reporter plasmid. The yeast *Saccharomyces cerevisiae* strain *EGY48* was used for transformation. Qualitative and quantitative β-galactosidase assays were performed according to the manufacturer's protocol using *O*-nitrophenyl β-D-galactopyranoside as a substrate (Clontech).

To determine the transcriptional activity of LTF1, we fused the coding sequence of *LTF1* in-frame with *VP16* (herpes simplex virus activation domain) by PCR to construct the *BD-LTF1-VP16* plasmid, which was transformed into yeast strain *AH109*. A β-galactosidase assay was performed as described above.

Subcellular Localization Assay

The *LTF1* coding sequence was amplified and cloned into the *pCAMBIA1300-35S-mCherry* vector (Gui et al., 2016) to obtain *LTF1-mCherry*, which was transformed into *A. tumefaciens* strain *GV3101* for transient transformation into tobacco (*Nicotiana benthamiana*). After 48 h of incubation, leaf cells were stained with the blue DNA-binding dye 4′,6-diamidino-2-phenylindole (DAPI), and mCherry and DAPI fluorescence was examined using a confocal microscope (LSM 510 META; Zeiss).

Immunoprecipitation and LC–MS/MS (IP–MS) Analysis

IP–MS was carried out as previously described (Gui et al., 2016). In brief, total proteins were extracted from *LTF1-3FLAG* transgenic plants using extraction buffer (50 mM Tris–HCl [pH 7.4], 150 mM NaCl, 5 mM $MgCl_2$, 1 mM EDTA, 1% Triton X-100, and 0.1% protease inhibitor cocktail [Promega]). The extracted proteins were incubated with pretreated anti-FLAG antibody-coupled agarose beads (Sigma). Beads were washed three times and eluted with 3FLAG peptide. The eluted proteins were enriched and digested by trypsin. The extracted peptides were concentrated, desalted, and analyzed using an LTQ Velos mass spectrometer (Thermo Scientific).

Protein Interaction Assays

The LTF1 C-terminal sequence (amino acids 151–268) fused to the *GAL4 DNA*-binding domain in the *pGBKT7* vector (Clontech) was used as bait in a yeast two-hybrid assay screen of a *Populus* developing xylem cDNA library developed in our laboratory. Yeast *AH109* cells containing the bait vector *BD-LTF1C* were further transformed with the *Populus* developing xylem cDNA library cloned into the prey vector *pACT* (Clontech), and selected on yeast synthetic dropout medium without Trp, Leu, and His, supplemented with 30 mM 3-AT.

For yeast two-hybrid confirmation, the full-length *LTF1* coding sequence was subcloned into the *pGADT7* vector (Clontech). *PdMPK6* and *PdMPK6-CA*, a constitutively active form of *PdMPK6*, were subcloned into the *pGBKT7* vector (Clontech). *AD-LTF1* was then co-transformed with *BD-PdMPK6* or *BD-PdMPK6-CA* into yeast strain *AH109* for further verification of the interaction.

For the BiFC assay, the *PdMPK6* and *LTF1* coding sequences were amplified and subcloned into the *pCAMBIA1300-35S-YN* and *pCAMBIA1300-35S-YC* plasmids (Gui et al., 2016), respectively. The resulting constructs were transformed into *A. tumefaciens* strain *GV3101* and transformed into *N. benthamiana* leaf cells, individually or combined, for BiFC analysis as previously described (Gui et al., 2016).

For the co-immunoprecipitation (Co-IP) assay, FLAG-tagged PdMPK6 and Myc-tagged LTF1 were expressed in tobacco. After 2 days of incubation, plant material was collected and ground in liquid nitrogen to a fine powder. Total proteins were extracted with extraction buffer (50 mM Tris–HCl [pH 7.4], 150 mM NaCl, 5 mM $MgCl_2$, 1 mM EDTA, 1% Triton X-100, and 1× protease inhibitor cocktail [Roche]) as previously described (Gui et al., 2016). Anti-FLAG antibody-coupled agarose beads (Sigma) were used to co-precipitate LTF1 with PdMPK6. The coIP and western blot assays were performed as previously described (Gui et al., 2016).

In Vivo and *In Vitro* Phosphorylation Assays

For the *in vivo* phosphorylation assays, the shoot tips of 2- and 8-month-old *LTF1OE* plants (LO23) were ground in liquid nitrogen to a fine powder.

Total proteins were extracted with a buffer (50 mM Tris–HCl [pH 7.4], 150 mM NaCl, 5 mM $MgCl_2$, 1 mM EDTA, and 1% Triton X-100) supplemented with 1× protease inhibitor cocktail (Roche) and 1× phosphatase inhibitor cocktail (Roche) for 30 min, and centrifuged at 4°C at 12 000 *g* for 15 min. The supernatant was incubated with pretreated anti-FLAG antibody-coupled agarose beads (Sigma) for 2 h at 4°C. Beads were washed three times with extraction buffer, and LTF1-3FLAG protein was eluted from the beads by competition with a 3× FLAG peptide. The eluted proteins were enriched using an ultrafiltration column with a nominal molecular weight limit of 3 kDa (Millipore) and were subjected to tryptic digestion (Promega). The digested peptides were further concentrated, desalted, and analyzed by nano-LC (Ultimate 3000, Dionex; trap column: Acclaim PePmap 100, 75 μm × 2 cm, nanoviper, C18, 3.0 μm, 100 A, Thermo Scientific; column: Venusil×BPC, C18, 5.0 μm, 150 A, Agela Technologies; eluent: 0.1% formic acid, 0%–80% acetonitrile) and analyzed by MS/MS (Q Exactive, Thermo Scientific). Database searches were carried out using a MS/MS ion search program (MASCOT, http://www.matrixscience.com) against the amino acid sequence of LTF1.

For the Phos-tag immunoblotting assay, proteins were extracted from 2-month-old (grown in a phytotron) and 8-month-old (grown in a glasshouse) transgenics. To block PdMPK6 activity, we treated *LTF1OE* plants with AG-126 (+: 50 μM, ++: 100 μM, −: 0 μM) for 2 h before protein extraction. Extracted proteins were separated in an 8% SDS–PAGE gel containing 50 μM Phos-tag (AAL-107; Wako, Japan) and 200 μM $MnCl_2$, following the manufacturer's instructions. LTF1 was detected with the anti-FLAG antibody (Abmart). For immunoblotting assays, phosphorylated MPKs were detected with the anti–Phospho-p44/p42 MAPK (anti-pTEpY) antibody (Cell Signaling Technologies) and PdMPK6 was detected with the anti-MPK6 antibody (Sigma).

For the *in vitro* phosphorylation assays, the full length coding sequences of WT *LTF1* and phosphorylation-null *LTF1* (*LTF1^{AA}*), as well as *PdMKK4^{DD}* (*T218D/S224D*), a constitutively active form of *PdMKK4*, were subcloned into the *pET28a*(+) vector (Novagen) for expression as a fusion protein with a His6 tag at the C terminus. *PdMPK6* was also subcloned into the *pGEX-6p-1* vector (GE Healthcare) for expression as a fusion protein with a glutathione *S*-transferase tag. These recombinant proteins were expressed and purified for use in the phosphorylation assay as previously described (Li et al., 2002), with minor modification. In brief, kinase assays were performed in protein kinase buffer (50 mM HEPES [pH 7.4], 10 mM $MgCl_2$, 1 mM DTT, 30 μM ATP) containing 10 μCi [γ-^{32}P]ATP and 1 μg of each protein. The reaction mixtures were incubated with protein at 30°C for 1 h. The kinase reaction was terminated by boiling with 5× SDS sample buffer for 5 min. Protein phosphorylation was analyzed by SDS–PAGE, and images were obtained by a Typhoon FLA 9000 phosphor imager (Amersham).

For *in vitro* examination of phosphorylation sites, LTF1 was incubated with or without PdMPK6/PdMKK4^{DD} in kinase buffer (50 mM HEPES [pH 7.4], 10 mM $MgCl_2$, 1 mM DTT, 30 μM ATP) at 30°C for 1 h. The reaction was stopped, and proteins were separated by SDS–PAGE and stained with Coomassie brilliant blue. The bands corresponding to LTF1 were excised for LC–MS/MS analysis to determine the phosphorylation sites.

Cell-Free Protein Degradation Assay

The cell-free protein degradation assay was performed as previously described (Wang et al., 2009) with slight modifications. In brief, total proteins were extracted from the developing xylem of *Populus* grown in a glasshouse at 8 months old with degradation buffer containing 25 mM Tris–HCl (pH 7.5), 10 mM NaCl, 10 mM $MgCl_2$, 5 mM DTT, and 10 mM ATP. The proteins in the supernatant were used for the LTF1 degradation assay. Five hundred micrograms of supernatant protein and 50 μM MG132 (Sigma) or 20 U of thermosensitive alkaline phosphatase (FastAP) (Thermo) were incubated with equal amounts of recombinant LTF1-3FLAG or LTF1^{AA}-3FLAG protein. After incubation at 22°C for 0.5, 1, 1.5, and 2 h, an immunoblotting experiment with LTF1-3FLAG or LTF1^{AA}-3FLAG was carried out using the anti-FLAG antibody (Abmart). For the plant-derived LTF1 protein, protein extracts from *LTF1-3FLAG* or *LTF1^{AA}-3FLAG* transgenic lines were used for the degradation assay.

SUPPLEMENTAL INFORMATION

Supplemental Information is available at *Molecular Plant Online*.

FUNDING

This work was supported by the Chinese Ministry of Science and Technology (grant no. 2016YFD0600104), the National Natural Science Foundation of China (grant nos. 31630014 and 31401301), the Chinese Ministry of Agriculture (grant no. 2018ZX08020002), the Youth Innovation Promotion Association CAS (grant no. 2017318), the Chinese Academy of Sciences (grant no. XDB27020104), the SANOFI-SIBS Scholarship Program, and the Shanghai Key Laboratory of Bio-Energy Crops.

AUTHOR CONTRIBUTIONS

J.G. and L.L. designed the research; J.G., L.F., Y.Z., and J.S. performed the research. J.G., L.F., T.U., and L.L. analyzed the data. J.G. and L.L. wrote the paper.

ACKNOWLEDGMENTS

We thank Dr. Ron Sederoff for critical reading and revision of the manuscript. We appreciate assistance from Dr. Wenli Hu for GC–MS analysis, Yuanhong Shan for LC–MS analysis, and Naixu Xu for assistance with the phosphorylation assay. No conflict of interest declared.

Received: March 5, 2019
Revised: May 1, 2019
Accepted: May 20, 2019
Published: May 27, 2019

REFERENCES

Asai, T., Tena, G., Plotnikova, J., Willmann, M.R., Chiu, W.L., Gomez-Gomez, L., Boller, T., Ausubel, F.M., and Sheen, J. (2002). MAP kinase signalling cascade in *Arabidopsis* innate immunity. Nature **415**:977–983.

Bhargava, A., Mansfield, S.D., Hall, H.C., Douglas, C.J., and Ellis, B.E. (2010). MYB75 functions in regulation of secondary cell wall formation in the *Arabidopsis* inflorescence stem. Plant Physiol. **154**:1428–1438.

Boerjan, W., Ralph, J., and Baucher, M. (2003). Lignin biosynthesis. Annu. Rev. Plant Biol. **54**:519–546.

Borevitz, J.O., Xia, Y., Blount, J., Dixon, R.A., and Lamb, C. (2000). Activation tagging identifies a conserved MYB regulator of phenylpropanoid biosynthesis. Plant Cell **12**:2383–2394.

Colcombet, J., and Hirt, H. (2008). *Arabidopsis* MAPKs: a complex signalling network involved in multiple biological processes. Biochem. J. **413**:217–226.

Fornale, S., Shi, X., Chai, C., Encina, A., Irar, S., Capellades, M., Fuguet, E., Torres, J.L., Rovira, P., Puigdomenech, P., et al. (2010). ZmMYB31 directly represses maize lignin genes and redirects the phenylpropanoid metabolic flux. Plant J. **64**:633–644.

Foster, C.E., Martin, T.M., and Pauly, M. (2010a). Comprehensive compositional analysis of plant cell walls (Lignocellulosic biomass) part I: lignin. J. Vis. Exp. https://doi.org/10.3791/1745.

Foster, C.E., Martin, T.M., and Pauly, M. (2010b). Comprehensive compositional analysis of plant cell walls (lignocellulosic biomass) part II: carbohydrates. J. Vis. Exp. https://doi.org/10.3791/1837.

Fraser, C.M., and Chapple, C. (2011). The phenylpropanoid pathway in *Arabidopsis*. *Arabidopsis* Book **9**:e0152.

Gui, J., Shen, J., and Li, L. (2011). Functional characterization of evolutionarily divergent 4-coumarate:coenzyme a ligases in rice. Plant Physiol. **157**:574–586.

Gui, J., Zheng, S., Liu, C., Shen, J., Li, J., and Li, L. (2016). OsREM4.1 interacts with OsSERK1 to coordinate the interlinking between abscisic acid and brassinosteroid signaling in rice. Dev. Cell **38**:201–213.

Hamel, L.P., Nicole, M.C., Sritubtim, S., Morency, M.J., Ellis, M., Ehlting, J., Beaudoin, N., Barbazuk, B., Klessig, D., Lee, J., et al. (2006). Ancient signals: comparative genomics of plant MAPK and MAPKK gene families. Trends Plant Sci. **11**:192–198.

Hanisch, U.K., Prinz, M., Angstwurm, K., Hausler, K.G., Kann, O., Kettenmann, H., and Weber, J.R. (2001). The protein tyrosine kinase inhibitor AG126 prevents the massive microglial cytokine induction by pneumococcal cell walls. Eur. J. Immunol. **31**:2104–2115.

Hu, W.J., Harding, S.A., Lung, J., Popko, J.L., Ralph, J., Stokke, D.D., Tsai, C.J., and Chiang, V.L. (1999). Repression of lignin biosynthesis promotes cellulose accumulation and growth in transgenic trees. Nat. Biotechnol. **17**:808–812.

Huang, C., Zhang, R., Gui, J., Zhong, Y., and Li, L. (2018). The receptor-like kinase AtVRLK1 regulates secondary cell wall thickening. Plant Physiol. **177**:671–683.

Jin, H., Cominelli, E., Bailey, P., Parr, A., Mehrtens, F., Jones, J., Tonelli, C., Weisshaar, B., and Martin, C. (2000). Transcriptional repression by AtMYB4 controls production of UV-protecting sunscreens in *Arabidopsis*. EMBO J. **19**:6150–6161.

Kubo, M., Udagawa, M., Nishikubo, N., Horiguchi, G., Yamaguchi, M., Ito, J., Mimura, T., Fukuda, H., and Demura, T. (2005). Transcription switches for protoxylem and metaxylem vessel formation. Genes Dev. **19**:1855–1860.

Le Gall, H., Philippe, F., Domon, J.M., Gillet, F., Pelloux, J., and Rayon, C. (2015). Cell wall metabolism in response to abiotic stress. Plants (Basel) **4**:112–166.

Lee, D., Meyer, K., Chapple, C., and Douglas, C.J. (1997). Antisense suppression of 4-coumarate:coenzyme A ligase activity in *Arabidopsis* leads to altered lignin subunit composition. Plant Cell **9**:1985–1998.

Lee, Y., Rubio, M.C., Alassimone, J., and Geldner, N. (2013). A mechanism for localized lignin deposition in the endodermis. Cell **153**:402–412.

Legay, S., Sivadon, P., Blervacq, A.S., Pavy, N., Baghdady, A., Tremblay, L., Levasseur, C., Ladouce, N., Lapierre, C., Seguin, A., et al. (2010). EgMYB1, an R2R3 MYB transcription factor from eucalyptus negatively regulates secondary cell wall formation in *Arabidopsis* and poplar. New Phytol. **188**:774–786.

Li, H., Ding, Y., Shi, Y., Zhang, X., Zhang, S., Gong, Z., and Yang, S. (2017). MPK3- and MPK6-mediated ICE1 phosphorylation negatively regulates ICE1 stability and freezing tolerance in *Arabidopsis*. Dev. Cell **43**:630–642.e4.

Li, J., Wen, J., Lease, K.A., Doke, J.T., Tax, F.E., and Walker, J.C. (2002). BAK1, an *Arabidopsis* LRR receptor-like protein kinase, interacts with BRI1 and modulates brassinosteroid signaling. Cell **110**:213–222.

Li, L., Zhou, Y., Cheng, X., Sun, J., Marita, J.M., Ralph, J., and Chiang, V.L. (2003). Combinatorial modification of multiple lignin traits in trees through multigene cotransformation. Proc. Natl. Acad. Sci. U S A **100**:4939–4944.

Li, S., Wang, W., Gao, J., Yin, K., Wang, R., Wang, C., Petersen, M., Mundy, J., and Qiu, J.L. (2016). MYB75 phosphorylation by MPK4 is required for light-induced anthocyanin accumulation in *Arabidopsis*. Plant Cell **28**:2866–2883.

Ma, X., Zhang, Q., Zhu, Q., Liu, W., Chen, Y., Qiu, R., Wang, B., Yang, Z., Li, H., Lin, Y., et al. (2015). A robust CRISPR/Cas9 system for convenient, high-efficiency multiplex genome editing in monocot and dicot plants. Mol. Plant **8**:1274–1284.

Mitsuda, N., Iwase, A., Yamamoto, H., Yoshida, M., Seki, M., Shinozaki, K., and Ohme-Takagi, M. (2007). NAC transcription factors, NST1 and NST3, are key regulators of the formation of secondary walls in woody tissues of *Arabidopsis*. Plant Cell **19**:270–280.

Morse, A.M., Whetten, R.W., Dubos, C., and Campbell, M.M. (2009). Post-translational modification of an R2R3-MYB transcription factor by a MAP Kinase during xylem development. New Phytol. **183**:1001–1013.

Moura, J.C., Bonine, C.A., de Oliveira Fernandes Viana, J., Dornelas, M.C., and Mazzafera, P. (2010). Abiotic and biotic stresses and changes in the lignin content and composition in plants. J. Integr. Plant Biol. **52**:360–376.

Osakabe, K., Tsao, C.C., Li, L., Popko, J.L., Umezawa, T., Carraway, D.T., Smeltzer, R.H., Joshi, C.P., and Chiang, V.L. (1999). Coniferyl aldehyde 5-hydroxylation and methylation direct syringyl lignin biosynthesis in angiosperms. Proc. Natl. Acad. Sci. U S A **96**:8955–8960.

Persak, H., and Pitzschke, A. (2013). Tight interconnection and multi-level control of *Arabidopsis* MYB44 in MAPK cascade signalling. PLoS One **8**:e57547.

Popescu, S.C., Popescu, G.V., Bachan, S., Zhang, Z.M., Gerstein, M., Snyder, M., and Dinesh-Kumar, S.P. (2009). MAPK target networks in *Arabidopsis thaliana* revealed using functional protein microarrays. Gene Dev. **23**:80–92.

Shen, H., He, X., Poovaiah, C.R., Wuddineh, W.A., Ma, J., Mann, D.G., Wang, H., Jackson, L., Tang, Y., Stewart, C.N., Jr., et al. (2012). Functional characterization of the switchgrass (*Panicum virgatum*) R2R3-MYB transcription factor PvMYB4 for improvement of lignocellulosic feedstocks. New Phytol. **193**:121–136.

Sonbol, F.M., Fornale, S., Capellades, M., Encina, A., Tourino, S., Torres, J.L., Rovira, P., Ruel, K., Puigdomenech, P., Rigau, J., et al. (2009). The maize ZmMYB42 represses the phenylpropanoid pathway and affects the cell wall structure, composition and degradability in *Arabidopsis thaliana*. Plant Mol. Biol. **70**:283–296.

Song, D.L., Gui, J.S., Liu, C.C., Sun, J.Y., and Li, L.G. (2016). Suppression of PtrDUF579-3 expression causes structural changes of the glucuronoxylan in populus. Front. Plant Sci. **7**:493.

Sultan, S.E. (2000). Phenotypic plasticity for plant development, function and life history. Trends Plant Sci. **5**:537–542.

Tamagnone, L., Merida, A., Parr, A., Mackay, S., Culianez-Macia, F.A., Roberts, K., and Martin, C. (1998). The AmMYB308 and AmMYB330 transcription factors from antirrhinum regulate phenylpropanoid and lignin biosynthesis in transgenic tobacco. Plant Cell **10**:135–154.

Vanholme, R., Demedts, B., Morreel, K., Ralph, J., and Boerjan, W. (2010). Lignin biosynthesis and structure. Plant Physiol. **153**:895–905.

Velez-Bermudez, I.C., Salazar-Henao, J.E., Fornale, S., Lopez-Vidriero, I., Franco-Zorrilla, J.M., Grotewold, E., Gray, J., Solano, R., Schmidt, W., Pages, M., et al. (2015). A MYB/ZML complex regulates wound-induced lignin genes in maize. Plant Cell **27**:3245–3259.

Wang, F., Zhu, D., Huang, X., Li, S., Gong, Y., Yao, Q., Fu, X., Fan, L.M., and Deng, X.W. (2009). Biochemical insights on degradation of *Arabidopsis* DELLA proteins gained from a cell-free assay system. Plant Cell **21**:2378–2390.

Wang, J.P., Matthews, M.L., Williams, C.M., Shi, R., Yang, C.M., Tunlaya-Anukit, S., Chen, H.C., Li, Q.Z., Liu, J., Lin, C.Y., et al.

(2018). Improving wood properties for wood utilization through multi-omics integration in lignin biosynthesis. Nat. Commun. **9**:1579.

Whetten, R., and Sederoff, R. (1995). Lignin biosynthesis. Plant Cell **7**:1001–1013.

Whitmarsh, A.J., and Davis, R.J. (2000). Regulation of transcription factor function by phosphorylation. Cell Mol. Life Sci. **57**:1172–1183.

Wilkins, O., Nahal, H., Foong, J., Provart, N.J., and Campbell, M.M. (2009). Expansion and diversification of the populus R2R3-MYB family of transcription factors. Plant Physiol. **149**:981–993.

Xie, M., Zhang, J., Tschaplinski, T.J., Tuskan, G.A., Chen, J.G., and Muchero, W. (2018). Regulation of lignin biosynthesis and its role in growth-defense tradeoffs. Front. Plant Sci. **9**:1427.

Yang, L., Zhao, X., Ran, L., Li, C., Fan, D., and Luo, K. (2017). PtoMYB156 is involved in negative regulation of phenylpropanoid metabolism and secondary cell wall biosynthesis during wood formation in poplar. Sci. Rep. **7**:41209.

Ye, Z.H., and Zhong, R. (2015). Molecular control of wood formation in trees. J. Exp. Bot. **66**:4119–4131.

Zhao, C., Wang, P., Si, T., Hsu, C.C., Wang, L., Zayed, O., Yu, Z., Zhu, Y., Dong, J., Tao, W.A., et al. (2017). MAP kinase cascades regulate the cold response by modulating ICE1 protein stability. Dev. Cell **43**:618–629.e5.

Zhong, R., Demura, T., and Ye, Z.H. (2006). SND1, a NAC domain transcription factor, is a key regulator of secondary wall synthesis in fibers of *Arabidopsis*. Plant Cell **18**:3158–3170.

Zhong, R., Lee, C., Zhou, J., McCarthy, R.L., and Ye, Z.H. (2008). A battery of transcription factors involved in the regulation of secondary cell wall biosynthesis in *Arabidopsis*. Plant Cell **20**:2763–2782.

Zhong, R., Richardson, E.A., and Ye, Z.H. (2007). The MYB46 transcription factor is a direct target of SND1 and regulates secondary wall biosynthesis in *Arabidopsis*. Plant Cell **19**:2776–2792.

Zhong, R., and Ye, Z.H. (2007). Regulation of cell wall biosynthesis. Curr. Opin. Plant Biol. **10**:564–572.

Zhou, J., Lee, C., Zhong, R., and Ye, Z.H. (2009). MYB58 and MYB63 are transcriptional activators of the lignin biosynthetic pathway during secondary cell wall formation in *Arabidopsis*. Plant Cell **21**:248–266.